Chapter 11
λ Ori: A Case Study in Star Formation

Robert D. Mathieu

11.1 Introduction

In previous chapters we have discussed the products of star formation, from binary stars to field stars to open clusters to the Milky Way itself. Now we turn to an overview of the star-forming regions themselves. I will begin with an intensive look into one star-forming region that has long been a favourite of mine, and then later in Chap. 12, I will give a more general overview of star-forming regions. The region for this in-depth look is the eponymous λ Orionis association, named for the brightest star in the head of Orion. It is not actually an extremely bright star (which often leads to jokes about Orion's intelligence). However the last laugh is Orion's, for λ Ori lies at the centre of one of the most spectacular shells in the IRAS 100 μm maps. λ Ori also drives a particularly beautiful Sharpless HII region. Finally, the λ Orionis region is important because the evidence suggests that a recent supernova has cleared much of the region of its natal gas. Thus λ Ori is a star-forming region that yields a final census of the outcome, and thus a near-final story of how the region evolved. Furthermore, the region is currently dissolving into the Galactic field, so that we are seeing the interface between star-forming regions and the disc of the Milky Way.

11.2 Overview

Figure 11.1 places the λ Orionis region in the setting of the nearby Galaxy, as revealed in IRAS 100 μm dust emission. Such emission generally traces the interstellar medium with temperatures >30 K. As this is significantly higher than the ambient 3 K cosmic microwave background, as well as dense molecular clouds heated only by cosmic rays ($\sim$10 K), this warm dust is strongly correlated with the presence of active star formation and the presences of luminous stars. The λ Ori star-forming region is

R.D. Mathieu (✉)
Department of Astronomy, University of Wisconsin, Madison, WI, USA
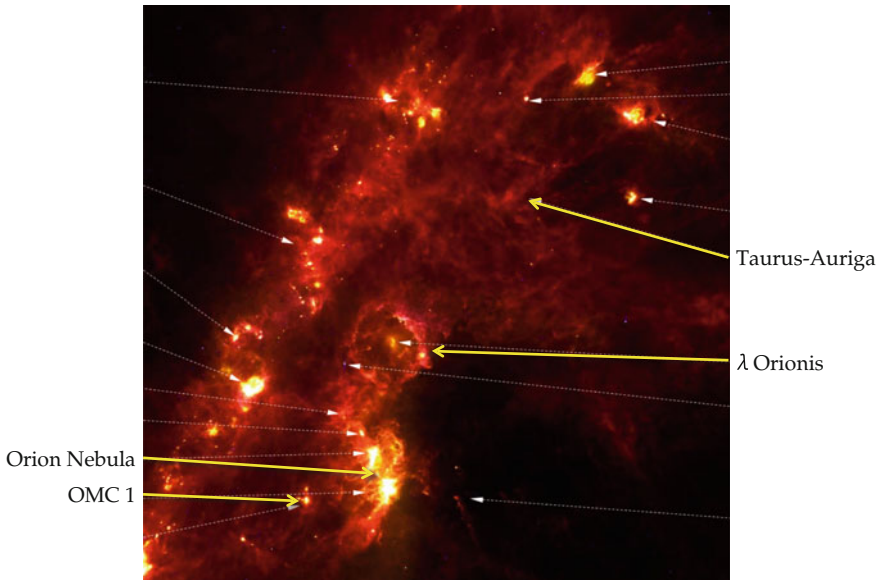e-mail: mathieu@astro.wisc.edu

Fig. 11.1 IRAS 100 μm map of the Galactic plane in the direction of the Orion molecular cloud. The Orion molecular cloud extends from λ Orionis to the lower edge of the image. Several star-forming regions are labelled, including the Taurus-Auriga clouds, the Orion Nebula and the OMC 1. Figure adapted from Bally (2008)

located at one end of the Orion giant molecular cloud. The region comprises several OB associations as identified by Adriaan Blaauw, with the hot and luminous Orion Nebula region particularly prominent at 100 μm. The region also includes numerous embedded star clusters and is littered with young low-mass stars throughout. For comparison, the Taurus-Auriga region is also identified. As discussed in Chap. 12, this region has proven seminal for our understanding of star formation, but Fig. 11.1 shows it to be a minor player on the Galactic scale.

Our exploration of the λ Ori region begins with a census of its contents. λ Ori itself is an O8 III star with a mass of roughly 10–15 $M_\odot$. λ Ori has a lower mass B0 V companion at a separation of 4.4 arcsec (or 1900 au in projection). Nine other B stars join λ Ori in a dense clump at the centre. Surrounding λ Ori is an ionisation-bounded HII region, 50 pc in diameter. Just beyond is a ring of neutral hydrogen and associated molecular clouds. Within this ring lie a large number of low-mass young stars, both classical T Tauri stars (with actively accreting circumstellar discs) and weak-lined T Tauri stars (with low accretion rates, traced by emission lines such as Hα, or no evidence at all for a circumstellar disc). FU Orionis is a member of the λ Ori region, and the namesake of a class of very-active young stellar objects characterised by high accretion rates. Finally there are several Herbig-Haro objects and quite a few jets and outflows. So there is star formation activity still underway, although as we shall see it is spatially limited by the recent dispersal of molecular gas and none is occurring near λ Ori itself. (For a more comprehensive discussion of the region see Mathieu

2008; for an overview of young stellar objects and important physical properties see Hartmann 1998.)

11.3 Dust and Molecular Gas

Currently the interstellar dust and molecular gas of the λ Ori region are located largely in the 60 pc diameter ring. Figure 11.2 shows this ring from three observational perspectives—dust extinction, thermal dust emission and molecular gas emission from rotational lines of carbon monoxide: the three closely trace each other.
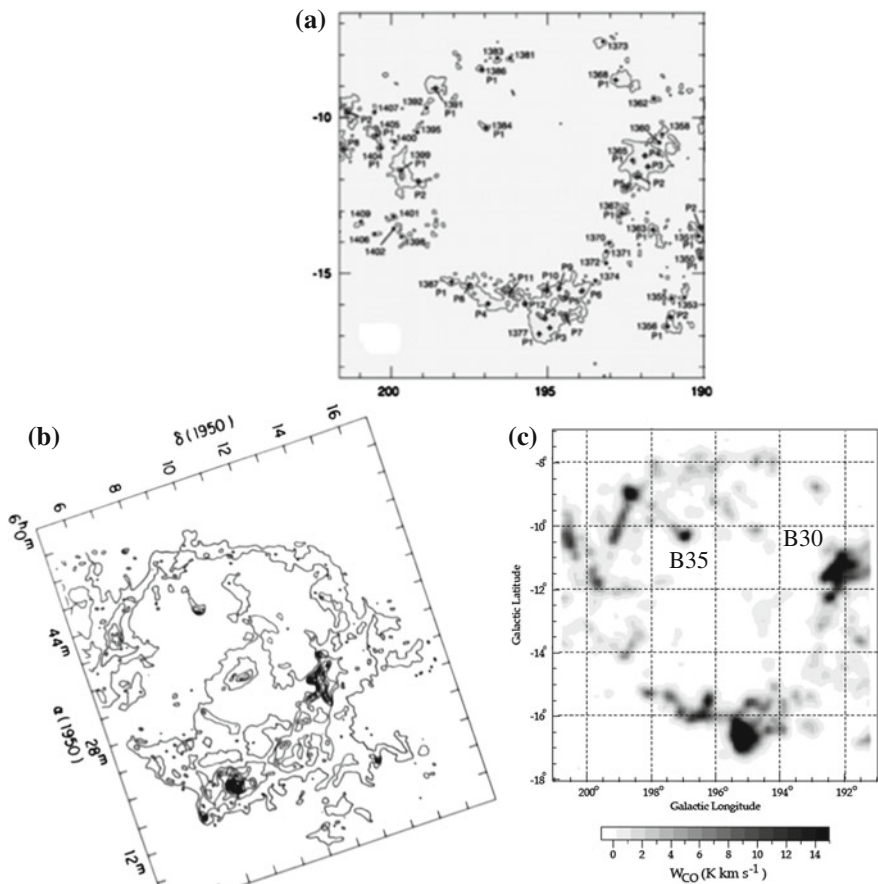

Fig. 11.2   a Extinction map of λ Ori region; *dots* are high extinction cores Dobashi et al. 2005. **b** IRAS 100 μm map. **c** CO (1-0) intensity map (Lang et al. 2000)

An early detection of the ring was made by Barnard, who identified numerous dark clouds in the region (Barnard 1919). The left, middle and right panels of Fig. 11.2 show an extinction map, an IRAS 100 μm map and a CO (1-0) intensity map of the λ Ori region from Dobashi et al. (2005), Maddalena and Morris (1987), Lang et al. (2000) respectively. Two dark clouds that will be particularly significant to our story, Barnard 30 and Barnard 35, are identified. The total molecular mass in the ring now is about 10^4 M$_\odot$, comparable to a giant molecular cloud at the smaller end of the mass range for these objects. The current mass is of course a lower limit on the original molecular gas mass. Interestingly there have been suggestions that the ring is expanding (Maddalena and Morris 1987), but at this point the kinematics remain uncertain.

11.4 Massive Stars

Analysis of the massive star population requires techniques of classical stellar astrophysics. Dolan and Mathieu (2001) used Strömgren photometry for 20 OB stars in the region to place them on a theoretical Hertzsprung-Russell diagram, shown in Fig. 11.3. The Strömgren technique uses a reddening-independent colour ratio to
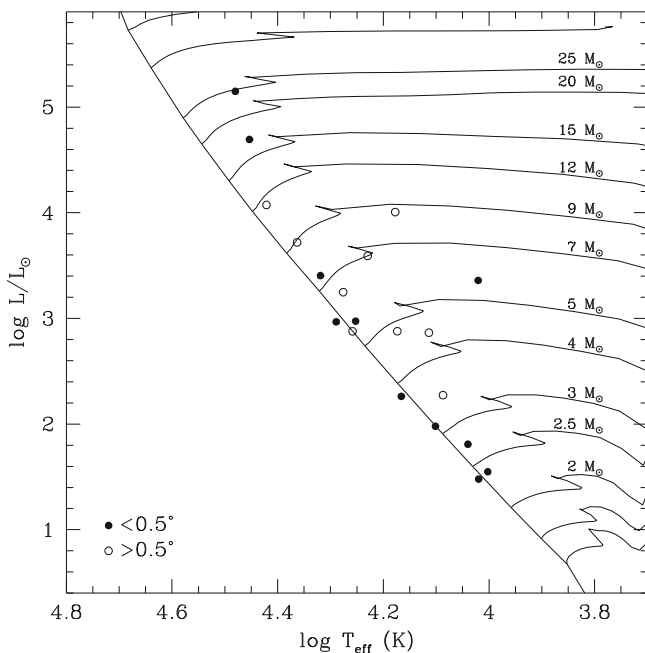

Fig. 11.3 Hertzsprung-Russell diagram of OB stars showing stars within 0.5° of λ Ori (*filled circles*) and more than 0.5° away (*open circles*). Also shown are evolutionary tracks from Schaller et al. (1992). Figure from Dolan and Mathieu (2001)

estimate the spectral type (thus permitting an estimate of extinction from comparison of expected colours to those observed), as well as constraints on surface gravity from measurement of Stark broadening from the Hβ index. The filled circles represent the stars in the central clump, with the two most luminous being λ Ori and its companion HD 36822; the open circles represent the more distributed stellar population.

Twelve of the 20 stars fit well to the theoretical main-sequence, suggestive of membership in the association. The two most luminous stars—λ Ori and HD 36822—are presumed members that have evolved off of the main-sequence, providing a clock with which to date the region as discussed below. The remaining 6 stars lie above the main-sequence by more than can be easily explained by binarity or evolution in a coeval stellar population. They may simply be foreground stars, although one of them—HD 36881—lies amidst the clump immediately around λ Ori. For the high-mass stars we have a good census of the products of this star-forming region, with the exception of yet more massive stars that have gone supernova.

11.5 Low-Mass Stars

Thus far, I have avoided using the phrase 'OB association' to describe the λ Ori star-forming region. With our ever increasing ability to discover young low-mass stars, it is clear that OB stars are simply the highly visible high-mass end of an IMF that almost always extends also to very-low stellar masses. I now introduce several ways that we can find low-mass stars in star-forming regions, using the λ Ori region as a case study.

11.5.1 Hα Emission and Objective Prism Surveys

Finding young low-mass stars through their strong Hα emission dates back to Haro and Herbig in the 1950s, long before it was known that the emission results from accretion from discs onto the pre-main-sequence (pre-MS) stars (see e.g. Haro 1953; Herbig 1954). Duerr et al. (1982) completed an objective prism survey of the entire λ Ori region. The filled circles in Fig. 11.4 show the union of classical T Tauri stars discovered both by these authors and Haro in an earlier study.

Interestingly, from the point of view of present and future synoptic studies, the vast majority of the stars found as Hα emitters are also known variable stars in the region. T Tauri stars as a class were identified in part through their variability by Joy (1945). Large amplitude irregular (and in some cases periodic rotation-related) accretion variability (>0.1 mag in the visible) is an efficient way to search for low-mass young stars. Lower amplitude periodic variability can also be used to measure rotation periods for young (and old) stars due to cool spots rotating on the stellar surface.
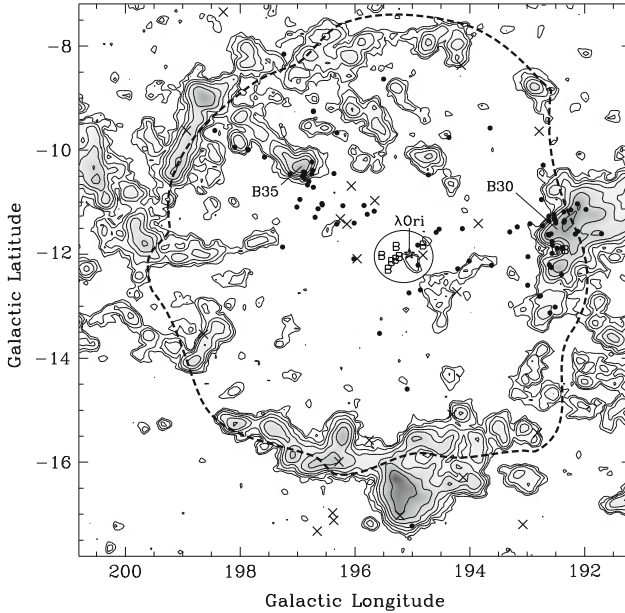
Fig. 11.4 The *filled circles* are Hα sources cataloged by Duerr et al. (1982). The *contours* are the CO (1-0) map of Lang and Masheder (1998), the *dashed line* delimits the HII region, and the 'B' symbols denote B stars near λ Ori. Figure from Dolan and Mathieu (1999)

Even though Duerr et al. (1982) surveyed the entire region, they only found classical T Tauri stars in a roughly linear domain extending from B35 to B30, about 50 pc in length. At about the same time, radio astronomers using millimetre wave molecular line observations were discovering that giant molecular clouds also tended to be elongated at about this scale in size. As a result, Duerr et al. (1982) conjectured that they were looking at a fossil giant molecular cloud within which the group of OB stars and low-mass stars had formed.

11.5.2 Lithium Absorption and Multi-Object Spectroscopic Surveys

In terms of obtaining a complete stellar census, a problem with Hα surveys is that they primarily reveal the classical T Tauri stars, whereas star-forming regions also have substantial populations of young low-mass stars that are not actively accreting. So how does one find all young low-mass stars in a systematic and unbiased way?

A characteristic property of young low-mass stars is presence of strong lithium (Li) absorption lines. Li is present in the photospheres of only young stars in cosmic abundances because it requires temperatures above $\simeq 3 \times 10^6$ K in order to be processed through nuclear reactions. Note this appears before central temperatures of $\simeq 10^7$ K are reached through pre-MS contractions (the onset of the main-sequence

where hydrogen burning is initiated). As young low-mass stars are nearly completely convective, the surface Li is brought deep below to the high temperature zones, burnt, and depleted from the surface photospheric abundances. Thus the resonant Li feature at 6708 Å is a diagnostic of youth, if one has the means to obtain a large number of intermediate-resolution spectra ($R > 3000$). Such spectra also provide estimates of surface gravity and heavy element abundance in addition to spectral type (i.e. temperature). If high enough resolution is obtained ($R > 10,000$) they also provide radial velocities, adding an additional kinematic dimension to membership determination.

This survey approach became feasible with the advent of large-N multi-object spectrographs. To give a sense of scale, the WIYN Observatory 3.5-m telescope with the Hydra multi-object spectrograph permits placement of nearly 100 optical fibres on stars within a 1°-diameter field-of-view. This proved a powerful capability for the WIYN Li survey to be discussed, but even so, the λ Ori region is of order 10° in diameter on the sky. A few multi-object spectrographs with larger fields-of-view and higher multiplex advantage have been commissioned in recent years.

Technically, a spectroscopic resolution of 20,000, or 15 km s^{-1}, suffices. Working in the 6640 Å spectral region provides Li 6708 Å, Hα, and a rich array of metal lines blueward of Hα for measuring radial velocities ($\sigma < 1$ km s^{-1}). Spectra with signal-to-noise yielding equivalent-width detection limits of order 0.1 Å suffice. None of
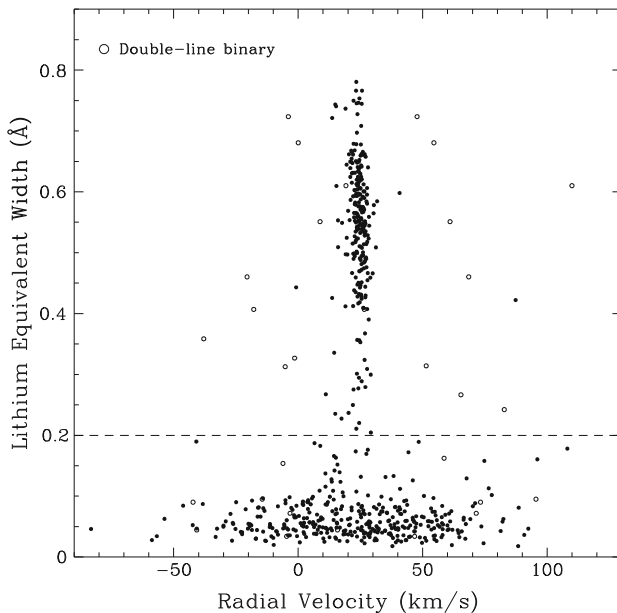

Fig. 11.5 Li line strength and radial velocity cleanly discriminate the low-mass pre-MS stars in the λ Ori star-forming region. Those stars with Li equivalent widths greater than 0.2 Å are taken to be members. These stars have a mean velocity of 24.5 km s^{-1}, similar to that of the Orion molecular cloud, and a velocity dispersion of only 2.3 km s^{-1}. Figure from Dolan and Mathieu (2001)
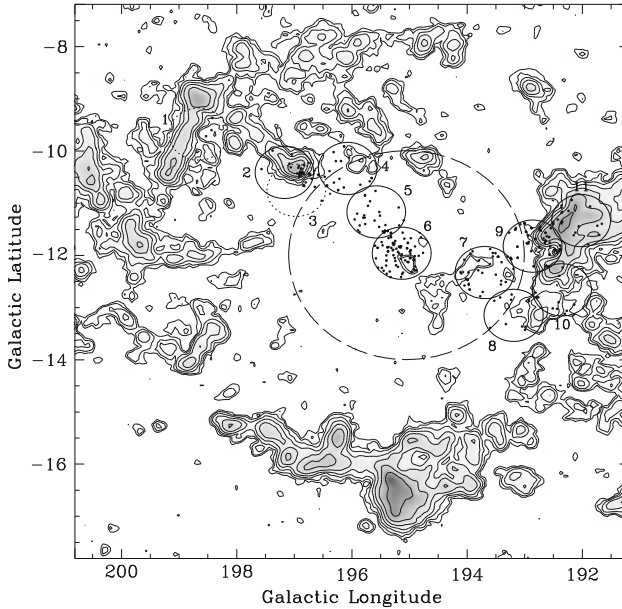
Fig. 11.6 *Smaller circles* are the target fields for the WIYN Li survey for young stars. The *filled dots* mark stars with strong Li absorption and radial velocities commensurate with the Orion region, and thus members of the λ Ori star-forming region. Compare to the Hα survey results in Fig. 11.4. Figure from Dolan and Mathieu (2001)

these specifications are particularly challenging; it is the wide-field large-N multi-object spectrograph that is the key.

Figure 11.5 shows a plot of Li equivalent width versus radial velocity for an unbiased population of late-type stars in the immediate vicinity of λ Ori. The separation between members of this star-forming region and the field is very clean in both dimensions: any star above 0.2 Å Li equivalent width appears to be a member and most have radial velocities consistent with Orion. In addition, if multi-epoch data are available the short-period pre-MS binaries can also be discerned. The 266 pre-MS stars revealed in Fig. 11.5 required about 4200 spectra of 3600 stars ($R < 16$ mag) obtained over the course of approximately 10 nights. The reward for this effort is shown in Fig. 11.6. The 1°-diameter regions surveyed with WIYN follow the linear extension revealed by the Hα surveys, but reveal nearly four times as many young low-mass stars. This unbiased (representative, but not complete) survey yields an estimate of the IMF and ultimately the star formation history of the region.

11.5.3 Photometric Surveys

Photometric surveys for young stars in associations rely on the over-luminosity of pre-MS stars compared to main-sequence stars. Figure 11.7 shows the deep $(RI)_c$
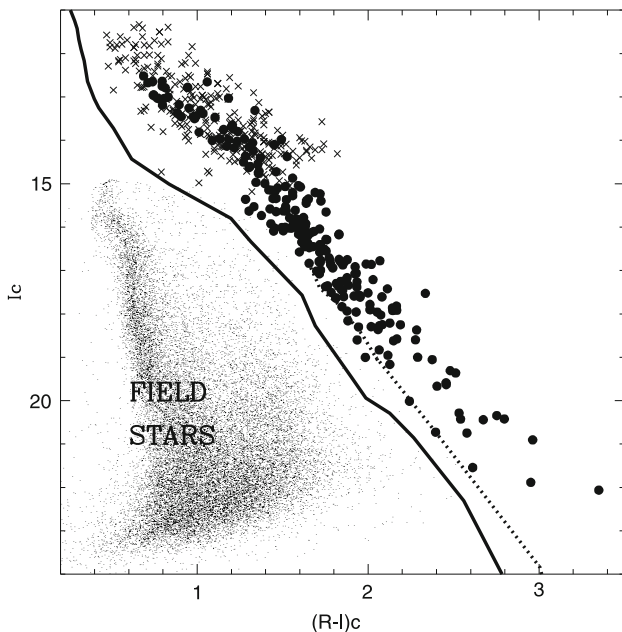
Fig. 11.7 Deep CMD for the field immediately around λ Ori. *Crosses* denote spectroscopically identified members, whereas *filled circles* represent photometrically identified candidate members. The *solid line* is the ZAMS and the *dotted line* is a 5 Myr isochrone both projected to the estimated distance of the region. Figure from Barrado y Navascués et al. (2004)

photometry of Barrado y Navascués et al. (2004) in the immediate vicinity of λ Ori. The solid line represents the zero-age main-sequence (ZAMS) at the Orion distance, while the dotted line is a 5 Myr isochrone; stars above the ZAMS are candidate association members. The separation of most field stars from the candidate members is good, but even so for any one candidate member another diagnostic of membership or youth is in order (e.g. follow-up spectroscopy). Another complication is the effect of interstellar reddening, making all objects appear redder and fainter than they are. In this CMD, the reddening vector is nearly parallel to the isochrones. Thus the age estimate may be valid, but the mass of the object is degenerate with the assumed stellar mass (in the absence of follow-up spectra). The beauty of this particular survey is its depth, reaching down to young brown dwarfs.

Wide-field photometric surveys are necessary to both obtain a global IMF for the region and to explore the spatial distribution of past star formation. Dolan and Mathieu (2002) performed a VRI photometric survey over the entire association, the results of which are shown in Fig. 11.8. In this study, after CMD selection a further statistical approach was taken to remove remaining field contamination, so the dots in Fig. 11.8 are 'proxy stars' representing over-densities of pre-MS stars. Despite
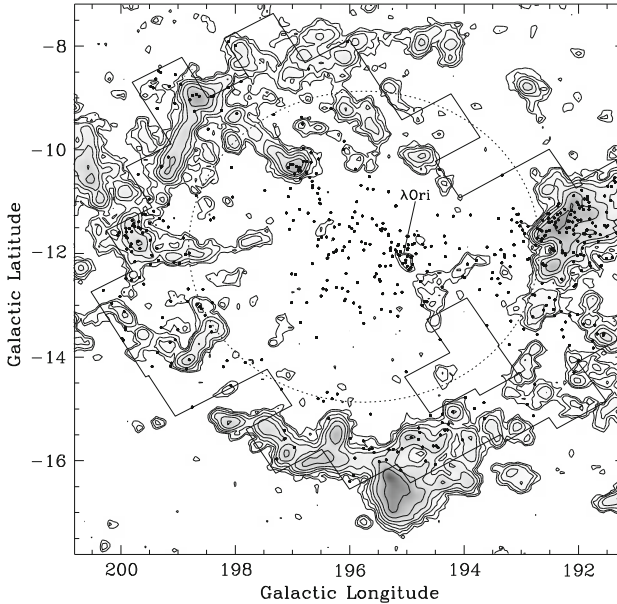
Fig. 11.8 Distribution of 'proxy' pre-MS stars based on optical photometry. The *solid outline* defines the domain of the survey. Note that fields outside the *dashed circle* are projected on the molecular clouds, so the surface densities are likely artificially enhanced by reddening. Figure from Dolan and Mathieu (2002)

surveying the entire region, there is very little evidence for prior star formation outside the linear region extending from B30 to B35.[1]

Very productive wide-field flux-limited surveys have also been performed at X-ray wavelengths. Young stars tend to have very active chromospheres, so that large X-ray luminosities (relative to the bolometric luminosities) are also an excellent diagnostic of youth. The ROSAT All-Sky Survey was able to detect young FGK stars within a couple of hundred parsecs while XMM-*Newton* and *Chandra* observations can detect much lower mass young stars as well as probe star-forming regions at greater distances (Barrado et al. 2011).

11.6 Analysis of a Star-Forming Region

Here we are using the λ Ori region as a tutorial case for a broad analysis of a star-forming region. Every region is unique and so no one region is truly an exemplar. And given the wonderful diversity of astrophysical phenomena in these regions no analysis can be comprehensive. Even so, this region is a good example of how surveys and analyses of star-forming regions are conducted.

---

[1] These photometric data were used to select out field stars from the target sample for the multi-object Li spectroscopy in Figs. 11.5 and 11.6.

11.6.1 Distance

The first thing we need is a reliable distance measurement. For the λ Ori region the photometric distance, which is to say main-sequence fitting to the more massive stars (see Fig. 11.3), remains the best measure at 450 ± 50 pc. This is comparable to the Orion molecular cloud, and so in conjunction with the kinematic (radial velocity) agreement an association of λ Ori with the much larger Orion molecular complex is likely. A more direct estimate of the distance to the Orion Nebula Cluster using VLBI astrometric measurements of masers with known velocities has yielded a distance consistent with the above. The OB stars are a bit far away for accurate and precise *Hipparcos* distances, although the measurements are formally consistent with the photometric distance. *Gaia* should finally provide excellent distances and hopefully three-dimensional structure.

11.6.2 Spatial Distribution of Star Formation

The λ Ori region is marked by the central clump of OB stars, with a radius of only about 2 pc. The compact spatial distribution of this clump is a very important clue to the evolution of the star-forming region. Whether determined from the associated low-mass stars or from *Hipparcos* proper motions, the velocity dispersion of the OB stars is $\simeq 2$ km s^{-1} in one dimension. This is typical of the internal motions of molecular clouds, but currently the only mass present is in the stars, and their mass is much too small to bind the system.[2] Thus on kinematic grounds alone this clump cannot have been unbound for more than $\simeq 1$ Myr.

The other clue from the spatial distribution is the roughly linear distribution of the lower-mass stars. They are not distributed throughout the ring, which implies that the ring was made *post facto*. We also have surface density enhancements of optically visible low-mass stars at B35 and B30, as well as several embedded sources in B35 indicating on-going star formation. As pointed out by Duerr et al. (1982), this spatial distribution of the low-mass stars suggests that they map out a previous giant molecular cloud.

11.6.3 Initial Mass Function

Young regions like λ Ori enable an almost 'pure' measurement of the IMF covering a broad range in mass and needing only modest corrections for the effects of stellar evolution for only the most massive stars. The IMF of the λ Ori region is interesting in several important ways. Figure 11.9 shows the IMF in the immediate vicinity of

---

[2]Just for a quick comparison, the old open cluster NGC 188 (see Chap. 8) has a total mass of about $1,000 \, M_\odot$ and a similar core radius, yet an internal velocity dispersion of only 0.4 km s^{-1}.
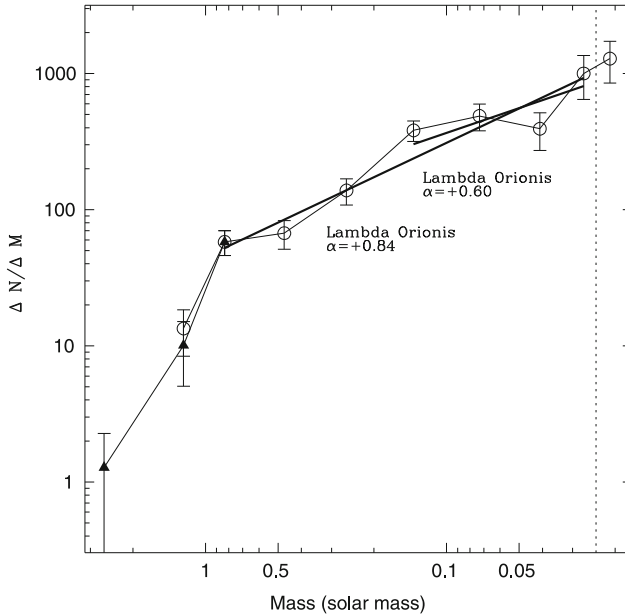
Fig. 11.9 IMF for the λ Ori star-forming region. *Filled triangles* denote data from Dolan and Mathieu (2001), whereas *open circles* represent data from Barrado y Navascués et al. (2004). The *vertical dashed line* represents the completeness limit of the Barrado y Navascués et al. study. The two power-law fits correspond to fits across different mass ranges, namely the stellar/substellar boundary (0.03–0.14 M$_\odot$; $\alpha = +0.6$) and the full sample (0.03–1 M$_\odot$; $\alpha = +0.86$). Figure from Barrado y Navascués et al. (2004)

λ Ori from Barrado y Navascués et al. (2004). Broadly speaking there is reasonable agreement between the IMF local to λ Ori and the field.

However, a detailed analysis shows important differences between local and global IMFs for the λ Ori region. Globally there are 107 stars throughout the region with masses between 0.4 and 0.9 M$_\odot$. Using the IMFs of Miller and Scalo (1979) or Kroupa et al. (1993) one would thus predict 10 or 19 OB stars in the region, respectively. In fact there are 16; so globally the IMF is as expected if drawn from that characterising the field (see e.g. Bastian et al. 2010). Interestingly, however, in the vicinity of λ Ori itself the number of low-mass stars is low by roughly a factor of two compared to the field, whereas away from λ Ori in the B30 and B35 regions the low-mass stars are over-populated by roughly a factor of three. Thus the global IMF of the λ Ori star-forming region resembles the field, while the local IMF appears to vary across the region. Perhaps it is the integration of the star formation process over the entire region that produces the field star IMF.

11.6.4 Total Stellar Population

The global stellar census yields a total mass in the region of all objects greater than $0.1\,M_\odot$ of $450–650\,M_\odot$. The current total molecular cloud mass is $10^4\,M_\odot$. Using this ratio, the global star formation efficiency in the region is very low, only a few percent. This is typical of star-forming regions. As discussed in Chap. 4, it is the local star formation efficiency which is most critical for determining whether a grouping of young stars is bound. Regrettably, we have no idea what was the mass of the dense core of the natal molecular cloud within which the OB stars likely formed, and so have no direct measure of the local star formation efficiency to compare with the global measure. However, combining information from spatial distributions and measured kinematics can place some constraints.

11.6.5 Accretion Disc Evolution

This topic is not central to the dynamics of star-forming regions, but is nonetheless an interesting outcome of the observations relevant to the initial conditions of planet formation. Furthermore, stellar dynamics might influence the structure and evolution of circumstellar discs. Recall that in the Li survey the spectra also included the Hα line, which for emission equivalent widths above 10 Å is taken as a proxy for active disc accretion. The presence of classical T Tauri stars with active accretion is evident near the dark clouds B35 and B30. On the other hand, there is a marked lack of Hα emission from the low-mass stars around the OB clump. Many of the Hα stars associated with B30 and B35 have ages similar to pre-MS stars found in the cluster near λ Ori. Dolan and Mathieu (2001) suggest that the absence of Hα emission from the central pre-MS stars is the result of an environmental influence linked to the luminous OB stars (for example external photoevaporation of the circumstellar gas in discs or dynamical interactions driving more rapid disc evolution). Similar results have been found for the λ Ori region with other accretion disc diagnostics (see e.g. Sacco et al. 2008; Barrado et al. 2011). Yet Hernández et al. (2009) find from deep *Spitzer* data that the frequency of accretion discs increases with lower stellar mass and argue for an evolutionary effect whereby the discs around lower-mass stars evolve more slowly than discs around higher-mass stars (cf. Hillenbrand et al. 1998; Carpenter et al. 2009).

11.6.6 Age Distribution

One of the reasons we embarked on a study of this star-forming region was to look for evidence of sequential star formation. For example, did a supernova from a star in the OB star clump accelerate star formation in the molecular clouds B30 and B35?
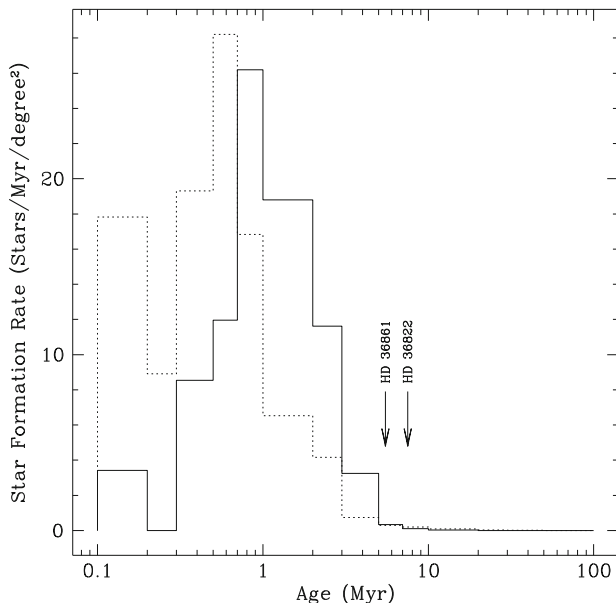
Fig. 11.10 Distribution of stellar ages for the low-mass pre-MS stars as estimated using the models of D'Antona and Mazzitelli (1998). The individual histograms are composed of stars within a 2° radius of λ Ori (*solid line*) and outside 2° (*dashed line*). The *arrows* mark the ages of the two evolved massive stars. Figure from Dolan and Mathieu (2001)

Strömgren photometry of the OB stars allows fairly precise age-dating of the two evolved OB stars, λ Ori and HD 36822. Pre-MS evolutionary tracks allow dating of the young solar-type stars, although the systematic uncertainties between sets of models are substantial. Dolan and Mathieu (2001) show the stellar age distributions for three sets of pre-MS models; for demonstration purposes one of these is shown Fig. 11.10, in which the D'Antona and Mazzitelli (1998) models were used to estimate individual stellar ages. For a detailed discussion of the pros and cons of various age-dating techniques the reader is referred to Soderblom (2010).

In the context of these models, there was a general onset of star formation in the region of the current OB star clump roughly 6–7 Myr ago. Both λ Ori and HD 36822 formed rather early in the story, and then there was a rapid rise in lower-mass star formation in the λ Ori vicinity. About 1 Myr ago the star formation in the λ Ori vicinity drops off precipitously. In the B30 and B35 regions the formation started later, peaked more recently (approximately a million years ago) and is still underway (as also evidenced by currently embedded stars in the clouds). The story is much the same using other models, but the time scales are different. As the OB stars and the solar-type stars are being dated using quite different astrophysics, it is not clear the absolute scales are comparable: it is difficult to rule out quantitatively one scenario or another. In any event, the evidence for sequential star formation in the region is not compelling. Yet, the evidence for star formation ending recently around the OB clump while still continuing in the remaining molecular clouds is stronger. Recall

that kinematic arguments suggest that the OB clump could not have lost its binding gas more than 1 Myr ago.

11.7 The Star Formation History of λ Ori

What story can be told for the λ Ori star-forming region inspired by this analysis? A possible scenario is presented schematically in Fig. 11.11. It begins with an elongated molecular cloud having several large-scale density enhancements. Roughly 6 Myr ago numerous OB stars were born in the central cloud but not elsewhere. Low-mass star formation began about the same time in all of the density enhancements, with a birth rate increasing gradually over several million years.

1 Myr ago a massive star in the OB clump went supernova, shredding the central cloud and thus unbinding the central stellar population. A ring of gas was pushed out from the central region, forming much of the ring seen today. (Importantly, Lang et al. 2000 argue that several massive clouds in the ring, such as B223, likely formed near their current locations.) Remnants of the adjacent dense clouds remain as B35 and B30; stars that had been formed within the forward edges of these dense clouds were exposed by the blast wave. Today we have star formation continuing in the remaining gas but it has ceased in the vicinity of the supernova epicentre.

Can we make any predictions concerning the future? The termination of star birth in B35 is 'imminent', as is the escape of the OB stars from their central position. All of the stars will disperse into the field over the next 10 Myr or so. The λ Ori
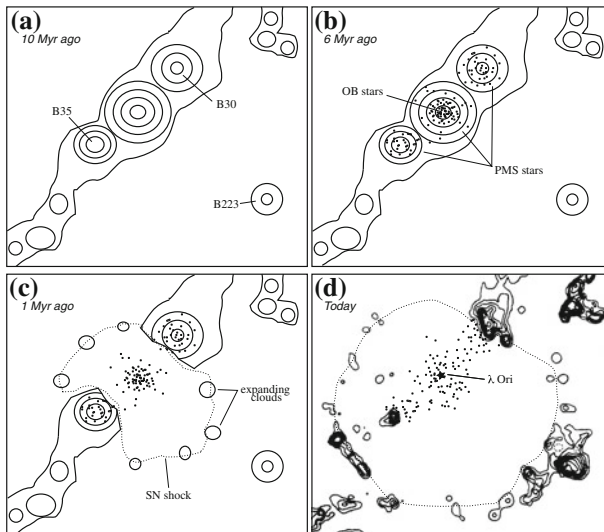

Fig. 11.11 Schematic history of the λ Ori star-forming region showing conditions at 10, 6 and 1 Myr ago, as well as a map of the molecular clouds today. Figure from Dolan and Mathieu (2002)

star-forming region will contribute field stars with an IMF similar to the current estimates, even though the IMF may have been inhomogeneous across the region. If *Gaia*'s successor observes this region 1 Myr from now, perhaps it will identify a remnant association of B stars with a paucity of lower-mass stars. It may also detect a more distributed complex of low-mass stars with similar space velocities, similar to what is known as the Ursa Majoris stream. Eventually the shear of the Galaxy will tear apart the moving group and the λ Ori star-forming region will have completed its contributions to the Galactic stellar population.

11.8 Final Thought

In terms of the dynamics and evolution of star-forming regions, the long-standing question of whether most stars form in OB associations or in T associations or in embedded clusters or in open clusters rests in part on distinctions derived from historical observational techniques. All stars are forming within giant molecular clouds that eventually disperse, leaving behind bound and unbound ensembles of stars across the entire IMF.

At the same time, there remain fundamental questions of star formation that are beyond the purview of this manuscript. I have suggested why star formation ended in the λ Orionis region, but have made no mention of why it started. The observations in hand are largely silent about the star formation rate and what determines it. While I have suggested that the IMF is not universal locally within the giant molecular cloud, nothing has been said about what in the star formation process determines stellar mass. The impact of these issues on the subject of this book remain to be seen.

References

Bally, J. 2008, Handbook of Star Forming Regions, Volume I: The Northern Sky, ed. B. Reipurth, ASP Monograph Publications, 459
Barnard, E. E. 1919, ApJ, 49, 1
Barrado, D., Stelzer, B., Morales-Calderón, M., et al. 2011, A&A, 526, 21
Barrado y Navascués, D., Stauffer, J. R., Bouvier, J., Jayawardhana, R., & Cuillandre, J.-C. 2004, ApJ, 610, 1064
Bastian, N., Covey, K. R., & Meyer, M. R. 2010, ARA&A, 48, 339
Carpenter, J. M., Bouwman, J., Mamajek, E. E., et al. 2009, ApJS, 181, 197
D'Antona, F. & Mazzitelli, I. 1998, in Astronomical Society of the Pacific Conference Series, Vol. 134, Brown Dwarfs and Extrasolar Planets, ed. R. Rebolo, E. L. Martin, & M. R. Zapatero Osorio, 442
Dobashi, K., Uehara, H., Kandori, R., et al. 2005, PASJ, 57, 1
Dolan, C. J. & Mathieu, R. D. 1999, AJ, 118, 2409
Dolan, C. J. & Mathieu, R. D. 2001, AJ, 121, 2124
Dolan, C. J. & Mathieu, R. D. 2002, AJ, 123, 387
Duerr, R., Imhoff, C. L., & Lada, C. J. 1982, ApJ, 261, 135

Haro, G. 1953, ApJ, 117, 73

Hartmann, L. 1998, Accretion Processes in Star Formation, ed. L. Hartmann, Cambridge University Press

Herbig, G. H. 1954, ApJ, 119, 483

Hernández, J., Calvet, N., Hartmann, L., et al. 2009, ApJ, 707, 705

Hillenbrand, L. A., Strom, S. E., Calvet, N., et al. 1998, AJ, 116, 1816

Joy, A. H. 1945, ApJ, 102, 168

Kroupa, P., Tout, C. A., & Gilmore, G. 1993, MNRAS, 262, 545

Lang, W. J. & Masheder, M. R. W. 1998, PASA, 15, 70

Lang, W. J., Masheder, M. R. W., Dame, T. M., & Thaddeus, P. 2000, A&A, 357, 1001

Maddalena, R. J. & Morris, M. 1987, ApJ, 323, 179

Mathieu, R. D. 2008, Handbook of Star Forming Regions, Volume I: The Northern Sky, ed. B. Reipurth, ASP Monograph Publications, 757

Miller, G. E. & Scalo, J. M. 1979, ApJS, 41, 513

Sacco, G. G., Franciosini, E., Randich, S., & Pallavicini, R. 2008, A&A, 488, 167

Schaller, G., Schaerer, D., Meynet, G., & Maeder, A. 1992, A&AS, 96, 269

Soderblom, D. R. 2010, ARA&A, 48, 581